Contemporary Mathematics
https://ojs.wiserpub.com/index.php/CM/

Research Article

Modeling Tick-Borne Zoonoses with Multi-Host and Multi-Vector Transmission Dynamics

Faraji Mohamed Tiraga[1,2], Kayode Oshinubi[2,3*], Tosin Samuel Osikoya[4], Sefinat Bola Jaiyeola[5], Michael Ojodomo Okone[6], Nebeolisa Ernest Onwuneme[7]

[1]Department of Mathematics and Statistics, College of Natural and Mathematical Sciences, University of Dodoma, Iyumbu, 41218, Tanzania
[2]School of Informatics, Computing, and Cyber Systems, Northern Arizona University, Flagstaff, AZ, United States
[3]Black in Mathematics Association, Pretoria, South Africa
[4]Department of Mathematics, Mathematics in Life Sciences Research Group, Technical University of Munich, Germany
[5]Department of Physical Sciences, Al-Hikmah University, Ilorin, Nigeria
[6]Department of Mathematics and Statistics, Texas A & M University-Corpus Christi, TX, USA
[7]University of L'Aquila, L'Aquila, Italy
E-mail: oshinubik@ieee.org

Received: 30 July 2025; **Revised:** 24 November 2025; **Accepted:** 10 December 2025

Abstract: Tick-borne zoonotic diseases pose an escalating global health threat, yet existing mathematical models often oversimplify the complex multi-host, multi-vector transmission dynamics, particularly neglecting non-viraemic (co-feeding) transmission and differential immunity mechanisms across species. We developed a novel compartmental model explicitly incorporating five transmission pathways: tick-to-human, animal-to-animal, animal-to-tick, tick-to-animal, and non-viraemic tick-to-tick transmission. The model uniquely captures transovarial transmission in ticks, species-specific immunity (permanent in animals, temporary in humans), and disease-induced mortality. Understanding how these multiple pathways interact is crucial for designing effective integrated control strategies targeting both vector and reservoir populations, particularly in regions experiencing ecological changes that favor tick proliferation. We derived the basic reproduction number R_0 and proved its positivity, showing that animal-to-animal transmission and non-viraemic tick transmission are the dominant drivers of disease persistence ($R_0 > 1$). Global stability analysis confirmed that the disease-free equilibrium is globally asymptotically stable when $R_0 < 1$. Sensitivity analysis revealed that reducing animal treatment time and limiting inter-animal contact have the greatest impact on reducing R_0. Our results demonstrate that tick control alone is insufficient; integrated strategies combining animal vaccination/treatment, movement restrictions, and tick population management are essential. The framework is adaptable to various tick-borne pathogens (Lyme disease, tick-borne encephalitis, Crimean-Congo hemorrhagic fever) and provides quantitative guidance for resource allocation in disease control programs.

***Keywords*:** Tick-Borne Diseases (TBDs), deterministic model, scenario analysis, tick-host interactions, mathematical epidemiology

MSC: 91A40, 00A71, 93D05

Copyright ©2026 Kayode Oshinubi, et al.
DOI: https://doi.org/10.37256/cm.7220268053
This is an open-access article distributed under a CC BY license
(Creative Commons Attribution 4.0 International License)
https://creativecommons.org/licenses/by/4.0/

1. Introduction

Tick-Borne Diseases (TBDs) are an increasing public health concern, particularly in temperate regions where the abundance and distribution of ticks are influenced by climatic, ecological, and anthropogenic factors. Ticks act as vectors for numerous pathogens affecting both humans and animals, with Lyme disease, caused by *Borrelia burgdorferi*, being one of the most well-known examples in the Northern Hemisphere [1–3]. These diseases, caused by various pathogens including viruses, bacteria, and protozoa, are primarily transmitted to humans and animals through the bites of infected ticks. Particularly, those of the *Ixodidae* (hard ticks) family play a crucial role in the epidemiology of these diseases. Through their blood-feeding behavior, ticks acquire pathogens from infected hosts and subsequently transmit them to new hosts during later feedings [4]. Pathogen transmission can also occur transovarially, from infected adult females to their offspring, thus sustaining infection cycles across tick generations [5]. Among the most significant Tick-Borne Diseases affecting humans are Lyme borreliosis, Tick-Borne Encephalitis (TBE), Crimean-Congo Hemorrhagic Fever (CCHF), Rickettsiosis, and Tularemia. These diseases often result in severe illness, long-term health complications, and even death in humans, while also causing considerable economic losses in livestock-dependent communities. The complex life cycle of ticks, their host-seeking behavior, and their role as disease vectors underscore the need for effective surveillance and control strategies [4, 6, 7].

Globally, Tick-Borne Diseases are difficult to control due to the complex interactions between vectors, hosts, and environmental factors. For instance, Lyme borreliosis accounts for more than 80% of all tick-borne disease cases in the United States, while Europe continues to experience thousands of cases of TBE annually [2]. Climate change, urbanization, and human encroachment into natural habitats further exacerbate the problem by expanding tick habitats and increasing human exposure.

Mathematical and statistical models have become indispensable tools for understanding the transmission dynamics of Tick-Borne Diseases and for evaluating control strategies [8–10]. Numerous modeling approaches have been employed, including deterministic compartmental models, stochastic simulations, spatial-temporal models, and hybrid techniques integrating environmental and ecological data [8, 10–12]. These studies have highlighted the influence of host movement, seasonal variability, coinfection dynamics, and vector competence on disease transmission, providing valuable insights into disease emergence and control. Deterministic and stochastic models have been used to capture both average dynamics and variability due to environmental and demographic stochasticity [13–15]. These models are increasingly coupled with spatial data and machine learning techniques to predict tick abundance and disease risk more accurately [16, 17].

Environmental variables such as temperature, humidity, and vegetation are crucial in shaping tick phenology and pathogen development rates [12, 18, 19]. For instance, warming temperatures due to climate change have expanded the geographic range of several tick species, particularly *Ixodes scapularis* [18, 19]. Other studies have emphasized the importance of host movement and seasonal changes in tick-host contact rates [20, 21].

In this study, we develop and analyze a compartmental model of a tick-borne zoonotic disease that integrates human, animal, and tick populations. The model reflects the distinct infection pathways among and between these populations and captures key biological processes, including vector-host interactions, vertical and horizontal transmission, and environmental influences. We conduct a thorough mathematical analysis of the model, establishing key properties such as the positivity and boundedness of solutions, as well as the existence and uniqueness of equilibria. We derive analytical conditions for disease-free and endemic equilibria. Furthermore, we compute the basic reproduction number R_0 to assess outbreak potential and investigate its epidemiological implications. A sensitivity analysis is performed to identify the most influential parameters driving disease spread. Finally, scenario-based simulations are conducted to explore the effects of varying key parameters on the disease dynamics, offering insights into potential control and mitigation strategies.

By integrating ecological realism with epidemiological theory, our work contributes to the growing literature on TBD modeling and provides a flexible framework applicable to multiple systems and settings. Also, our work contributes to the growing body of research on vector-borne diseases by offering a comprehensive framework that can be adapted to specific tick-borne pathogens and ecological contexts. The modeling approach and findings presented herein may support public health authorities and ecologists in designing more effective interventions to curb the spread of Tick-Borne Diseases.

This study makes the following key contributions to tick-borne disease modeling: (1) Development of a novel multi-host, multi-vector compartmental model incorporating five distinct transmission pathways, including non-viraemic (co-feeding) transmission among ticks; (2) Integration of transovarial transmission in ticks and differential immunity assumptions (permanent in animals, temporary in humans); (3) Derivation of analytical expressions for the basic reproduction number (R_0) with explicit characterization of each transmission pathway's contribution; (4) Comprehensive sensitivity and scenario analyses identifying key parameters for targeted interventions.

The remainder of this paper is organized as follows: Section 2 presents the mathematical model formulation and assumptions. Also, we provide rigorous mathematical analysis, including uniqueness, positivity, equilibrium points, computation of R_0, and global stability analysis. Section 3 presents numerical simulations exploring model dynamics under various scenarios. Section 4 discusses sensitivity and scenario analyses with contour plots of R_0. Finally, Section 5 and Section 6 provide discussion, conclusions, and future research directions.

2. Methods

2.1 *Mathematical model*

The model we developed in this article takes into consideration the three populations (human, tick, and animal) of tick-borne disease, which are based on different infection pathways. The total human population at time t, denoted by $N_H(t)$, is subdivided into healthy but susceptible humans $S_H(t)$, exposed humans $E_H(t)$, infectious humans $I_H(t)$, treated humans $T_H(t)$, dead humans $D_H(t)$, and recovered humans $R_H(t)$. So, the total human population is given by

$$N_H(t) = S_H(t) + E_H(t) + I_H(t) + T_H(t) + D_H(t) + R_H(t).$$

The tick population is subdivided into four compartments: larvae $L_T(t)$, susceptible $S_T(t)$, exposed $E_T(t)$, and infectious $I_T(t)$, such that the total mammal population is given by

$$N_T(t) = L_T(t) + S_T(t) + E_T(t) + I_T(t).$$

We didn't consider recovered or dead ticks because their life span is short, which is about two to three years.

The animal population follows the same type of compartment as humans, which in this case the total population at time t, denoted by $N_A(t)$, is subdivided into healthy but susceptible animals $S_A(t)$, exposed humans $E_A(t)$, infectious humans $I_A(t)$, treated animals $T_A(t)$, dead animals $D_A(t)$, and recovered animals $R_A(t)$. So, the total animal population is given by

$$N_A(t) = S_A(t) + E_A(t) + I_A(t) + T_A(t) + D_A(t) + R_A(t).$$

The total population considered in the model dynamics is given as

$$N(t) = N_H(t) + N_T(t) + N_A(t).$$

Thus, the transmission model is represented by the following system of non-linear ordinary differential equations:

$$
\begin{cases}
\dfrac{dS_H}{dt} = \Lambda_H - (\mu_H + r\beta_4 I_T)S_H + aR_H \\
\dfrac{dE_H}{dt} = r\beta_4 I_T S_H - \delta_H E_H \\
\dfrac{dI_H}{dt} = \delta_H E_H - \alpha_H I_H \\
\dfrac{dT_H}{dt} = (1-P_H)\alpha_H I_H - (\rho_H + \gamma_H)T_H \\
\dfrac{dR_H}{dt} = P_H \alpha_H I_H + \gamma_H T_H - aR_H \\
\dfrac{dD_H}{dt} = \rho_H T_H \\
\dfrac{dL_T}{dt} = \Lambda_T - \Lambda_0 L_T \\
\dfrac{dS_T}{dt} = \Lambda_0 L_T - (\mu_T + \beta_3 I_A + \theta I_T + \lambda I_T)S_T \\
\dfrac{dE_T}{dt} = (\beta_3 I_A + \theta I_T + \lambda I_T)S_T - \delta_T E_T \\
\dfrac{dI_T}{dt} = \delta_T E_T - bI_T \\
\dfrac{dS_A}{dt} = \Lambda_A - (\mu_A + r\beta_1 I_T + \beta_2 I_A)S_A + cR_A \\
\dfrac{dE_A}{dt} = (r\beta_1 I_T + \beta_2 I_A)S_A - \delta_A E_A \\
\dfrac{dI_A}{dt} = \delta_A E_A - \alpha_A I_A \\
\dfrac{dT_A}{dt} = (1-P_A)\alpha_A I_A - (\rho_A + \gamma_A)T_A \\
\dfrac{dR_A}{dt} = P_A \alpha_A I_A + \gamma_A T_A - cR_A \\
\dfrac{dD_A}{dt} = \rho_A T_A
\end{cases}
\tag{1}
$$

under the following initial conditions:

$$S_H(0) > 0,\ E_H(0) \geq 0,\ I_H(0) \geq 0,\ T_H(0) \geq 0,\ D_H(0) \geq 0,\ R_H \geq 0,\ L_T \geq 0,\ S_T \geq 0,\ E_T \geq 0,\ I_T \geq 0,$$

$$S_A(0) > 0,\ E_A(0) \geq 0,\ I_A(0) \geq 0,\ T_A(0) \geq 0,\ D_A(0) \geq 0,\ R_A \geq 0,$$

with $(S_H(0), E_H(0), I_H(0), T_H(0), D_H(0), R_H(0), L_T(0), S_T(0), E_T(0), I_T(0), S_A(0), E_A(0), I_A(0), T_A(0), D_A(0), R_A(0)) \in R^{16_+}$.

The effective contact rate with an infectious tick or infectious animal is defined as:

$$\lambda_H = \frac{r\beta_4 I_T S_H}{N_H},\ \lambda_T = \frac{(\beta_3 I_A + \theta I_T + \lambda I_T) S_T}{N_T},\ \lambda_A = \frac{(r\beta_1 I_T + \beta_2 I_A) S_A}{N_A}.$$

The schematic diagram of the model is presented in Figure 1, and the parameters of Model (1) are described in Table 1).

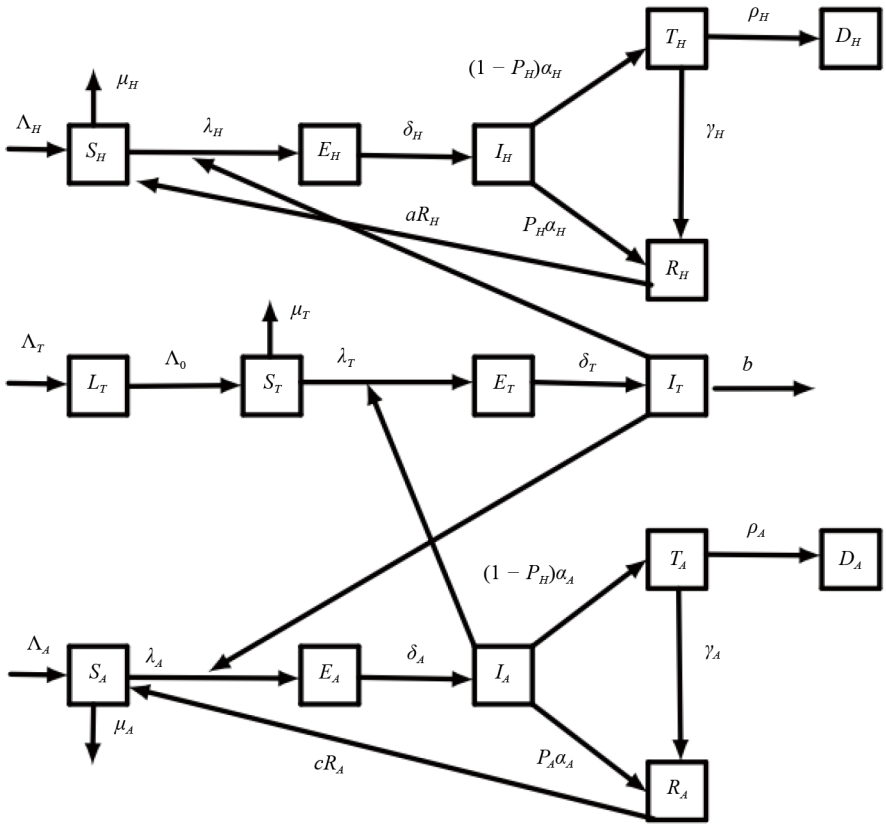


Figure 1. The schematic diagram for the mathematical model of tick-borne disease

Table 1. Description of parameters used in the model (1)

Parameters	Definition
Λ_H	Recruitment rate for human population
Λ_A	Recruitment rate for animal population
μ_H	Natural death rate of the human population
r	Tick bite rate
β_1	Transmission rate between tick and animal due to a bite
β_2	Transmission rate between animals when there is contact between an infected animal
β_3	Transmission rate between animal and tick when a tick bites an animal and becomes infected
β_4	Transmission rate between tick and human due to a bite
a	Human reinfection rate
b	Death rate due to the disease in tick
c	Animal reinfection rate
γ_H	Recovery rate for human that are treated
γ_A	Recovery rate for animal that are treated
δ_H	Incubation period for human
α_H	Treatment rate for human
ρ_H	Death rate due to the disease in human
Λ_T	Recruitment rate for larvae tick population
Λ_0	Transition from the larvae tick population to adult tick population
μ_T	Tick adult mortality rate
μ_A	Mortality rate of animal population
θ	The rate of non-viraemic transmission between co-feeding ticks
λ	The rate an infected adult female tick reproduces
P_A	Recovery rate for infected animal
P_H	Recovery rate for infected human
α_A	Treatment rate for animal
δ_A	Incubation period for animal
δ_T	Incubation period for tick
ρ_A	Death rate due to the disease in animal

The model assumptions are as follows:

• We assumed in our model that there are five pathways of transmission dynamics: non-viraemic or non-systematic transmission between ticks, animal-to-animal transmission, tick-to-human transmission, animal-to-tick transmission, and tick-to-animal transmission.

• We also assume that recovered animals may develop permanent immunity (or quasi-permanent immunity) but immunity wanes in a small fraction of the animal population due to immunosenescence in aging animals, immunocompromised individuals within the population and pathogen strain variation allowing partial immune escape to the disease, while humans are not permanently immune because they can be reinfected, and there is no recovery for infected ticks since ticks have a short life span.

• We assume there exists transovarial transmission among ticks (transmission from adult female tick to larvae); there is non-viraemic transmission amongst the tick (that is, susceptible ticks can be infected through co-feeding with an infected tick).

• We assumed that animals can infect another animal either through ingested feces or through shedding/contact with other animals during movement from one place to another and the tendency to split their time in different parts of the environment.

2.2 *Analysis of the model*

2.2.1 *Uniqueness*

Consider the general form of Ordinary Differential Equation (ODE) $y' = g(x, y)$ with the initial condition that $y(x_0) = y_0$. If g is continuous and has partial derivatives that are also continuous in the space $\mathscr{R}$, then $g(x, y)$ is Lipschitz.

We rewrite system (1) in the form of $G(x)$ with solution $x \in \mathbf{R}^{16}$.

$$
\begin{cases}
G_1 = \Lambda_H - (\mu_H + r\beta_4 I_T)S_H + aR_H \\
G_2 = r\beta_4 I_T S_H - \delta_H E_H \\
G_3 = \delta_H E_H - \alpha_H I_H \\
G_4 = (1 - P_H)\alpha_H I_H - (\rho_H + \gamma_H)T_H \\
G_5 = P_H \alpha_H I_H + \gamma_H T_H - aR_H \\
G_6 = \rho_H T_H \\
G_7 = \Lambda_T - \Lambda_0 L_T \\
G_8 = \Lambda_0 L_T - (\mu_T + \beta_3 I_A + \theta I_T + \lambda I_T)S_T \\
G_9 = (\beta_3 I_A + \theta I_T + \lambda I_T)S_T - \delta_T E_T \\
G_{10} = \delta_T E_T - (\beta_4 + \beta_1)I_T \\
G_{11} = \Lambda_A - (\mu_A + r\beta_1 I_T + \beta_2 I_A)S_A + cR_A \\
G_{12} = (r\beta_1 I_T + \beta_2 I_A)S_A - \delta_A E_A \\
G_{13} = \delta_A E_A - \alpha_A I_A \\
G_{14} = (1 - P_A)\alpha_A I_A - (\rho_A + \gamma_A)T_A \\
G_{15} = P_A \alpha_A I_A + \gamma_A T_A - cR_A \\
G_{16} = \rho_A T_A
\end{cases}
\tag{2}
$$

Theorem 1 The system (2) has a unique solution if $G(x)$ is continuous and has continuous partial derivatives.
Proof. Some partial derivatives of $G(x)$ are given below

$$\frac{\partial G_1}{\partial x_1} = |-(\mu_H + r\beta_4 I_T)| < \infty, \ \frac{\partial G_1}{\partial x_2} = 0 < \infty, \ \frac{\partial G_1}{\partial x_3} = 0 < \infty,$$

$$\frac{\partial G_1}{\partial x_4} = 0 < \infty, \ \frac{\partial G_1}{\partial x_5} = a < \infty, \ \frac{\partial G_1}{\partial x_6} = 0 < \infty, \ \frac{\partial G_1}{\partial x_7} = 0 < \infty,$$

$$\frac{\partial G_1}{\partial x_8} = 0 < \infty, \ \frac{\partial G_1}{\partial x_9} = 0 < \infty, \ \frac{\partial G_1}{\partial x_{10}} = r\beta_4 S_H < \infty,$$

$$\frac{\partial G_1}{\partial x_{11}} = 0 < \infty, \ \frac{\partial G_1}{\partial x_{12}} = 0 < \infty, \ \frac{\partial G_1}{\partial x_{13}} = 0 < \infty, \ \frac{\partial G_1}{\partial x_{14}} = 0 < \infty,$$

$$\frac{\partial G_1}{\partial x_{15}} = 0 < \infty, \ \frac{\partial G_1}{\partial x_{16}} = 0 < \infty.$$

The rest of the partial derivatives exist, are continuous, and are bounded in the space $\mathbf{R}^{16}$. Thus the solution exist. For uniqueness, let x_1^* and x_2^* be two solutions of model (1) such that

$$G_1(x_1^*) = \Lambda_H - (\mu_H + r\beta_4 I_T)S_{H_1} + aR_H$$

$$G_1(x_2^*) = \Lambda_H - (\mu_H + r\beta_4 I_T)S_{H_2} + aR_H.$$

Then

$$\begin{aligned} |G_1(x_1^*) - G_1(x_2^*)| &= |-(\mu_H + r\beta_4 I_T)(S_{H_1} - S_{H_2})| \\ &\leq |-(\mu_H + r\beta_4 I_T)||S_{H_1} - S_{H_2}| \\ &= L|x_1^* - x_2^*| \end{aligned}$$

Satisfying the Lipschitz condition with a Lipschitz constant $L = \mu_H + r\beta_4 I_T$. Thus, system (2) has a unique solution. □

2.2.2 *Conservation of non-negativity*

We show that the system (1) is epidemiologically and mathematically well-posed in the positive invariant region:

$$\mathbf{S} = \Big\{ S_H(t), E_H(t)), I_H(t), T_H(t), D_H(t), R_H(t), L_T(t), S_T(t), E_T(t), I_T(t), S_A(t), E_A(t),$$

$$I_A(t), T_A(t), D_A(t),\ R_A(t) \in \mathbf{R}_+^{16} : N_H(t) \leq \frac{\Lambda_H}{\mu_H}, N_T(t) \leq \frac{\Lambda_T}{\mu_T}, N_A(t) \leq \frac{\Lambda_A}{\mu_A} \Bigg\}$$

Theorem 2 There exists a domain **S** in which the solution $(S_H(t), E_H(t))$, $I_H(t)$, $T_H(t)$, $D_H(t)$, $R_H(t)$, $L_T(t)$, $S_T(t)$, $E_T(t)$, $I_T(t)$, $S_A(t)$, $E_A(t)$, $I_A(t)$, $T_A(t)$, $D_A(t)$, $R_A(t)$) is contained and bounded.

Proof. We prove this theorem using the idea of Tiraga et al. [22]. Let $S_H(t), E_H(t), I_H(t), T_H(t), D_H(t), RH(t), S_T(t)$, $L_T(t), E_T(t), I_T(t), S_A(t), E_A(t), I_A(t), T_A(t), D_A(t), R_A(t)$ be the any solution of system (1) with the initial conditon.

Then adding equation (1)-(6) of (1) of human population $(N_H(t))$ with assumption that in all compartments there is a natural death rate μ_H we get

$$\frac{N_H(t)}{dt} = \Lambda_H - \mu_H N_H(t) \tag{3}$$

Solving equation (3), we obtain $0 \leq N_H(t) \leq \left(N_H(0) - \frac{\Lambda_H}{\mu_H}\right) e^{-\mu_H t}$. It follows that as $t \mapsto \infty$, $N_H(t) \leq \frac{\Lambda_H}{\mu_H}$.

Similarly, for tick population, $N_T(t) \leq \frac{\lambda_T}{\mu_T}$ and animal population, $N_A(t) \leq \frac{\lambda_A}{\mu_A}$.

Therefore, **S** is positively invariant and attractive and the system (1) is mathematically well-posed and epidemiologically reasonable. □

2.2.3 *Analysis of steady states in the model*

The disease-free equilibrium point E_0 is the condition in which a tick-borne zoonotic disease does not persist in the system. To obtain E_0 we equate all the differential equations in the model to zero and put all the infection-related terms to zero $(S_H^0, E_H^0, I_H^0, T_H^0, D_H^0, R_H^0, L_T^0, S_T^0, E_T^0, I_T^0, S_A^0, E_A^0, I_A^0, T_A^0, D_A^0)$.

Thus gives:

$$(S_H^0, 0, 0, 0, 0, 0, L_T^0, S_T^0, 0, 0, S_A^0, 0, 0, 0, 0, 0)$$

where $S_H^0 = \frac{\Lambda_H}{\mu_H}, L_T^0 = \frac{\Lambda_T}{\Lambda_0}, S_T^0 = \frac{\Lambda_T}{\mu_T}, S_A^0 = \frac{\Lambda_A}{\mu_A}$.

Endemic equilibrium signifies the permanent existence of tick-borne diseases among the populations considered in this work. To obtain the endemic equilibrium, the state variables in the differential equations in model (1) must not be equal to zero and solving them simultaneously give the endemic equilibrium point as

$$(S_H^*, E_H^*, I_H^*, 0, R_H^*, 0, L_T^*, S_T^*, 0, I_T^*, S_A^*, E_A^*, I_A^*, 0, 0, 0)$$

where

$$S_H^* = \frac{\Lambda_H}{\mu_H}$$

$$E_H^* = \frac{r\beta_4\Lambda_H}{\delta_H\mu_H}(\beta_3 + \beta_2\Lambda_H - \alpha_A\mu_A)$$

$$I_H^* = \frac{r\beta_4\Lambda_H}{\alpha_H\mu_H}(\beta_3 + \beta_2\Lambda_H - \alpha_A\mu_A)$$

$$R_H^* = \frac{P_H r\beta_4\Lambda_H}{\mu_H a}(\beta_3 + \beta_2\Lambda_H - \alpha_A\mu_A)$$

$$L_T^* = \frac{\Lambda_T}{\Lambda_0}$$

$$S_T^* = \frac{\Lambda_T}{\mu_T}$$

$$I_T^* = \beta_3 + \beta_2\Lambda_H - \alpha_A\mu_A$$

$$S_A^* = \frac{\Lambda_A}{\mu_A}$$

$$E_A^* = \frac{-\alpha_A}{\delta_A}(\theta + \lambda + r\beta_1\Lambda_A)$$

$$I_A^* = -(\theta + \lambda + r\beta_1\Lambda_A)$$

2.2.4 *Basic reproduction number*

The fundamental reproduction number R_0 is a critical epidemiological metric that quantifies the average number of secondary infections induced by a single infected individual in a completely susceptible population [23]. It is employed to evaluate the potential for the transmission of an infectious disease and to direct public health interventions.

We employ the next-generation matrix approach to calculate the basic reproduction number. This approach encompasses the transmission matrix F (new infections) and the transition matrix V (movement of individuals out of the infected compartments) [22–24]. The model (1) comprises six contaminated compartments: E_H, I_H, E_T, I_T, E_A, and I_A.

Then, matrix F and V are given by

$$F = \begin{bmatrix} 0 & 0 & 0 & \frac{\Lambda_H\beta_4 r}{\mu_H} & 0 & 0 \\ 0 & 0 & 0 & 0 & 0 & 0 \\ 0 & 0 & 0 & \frac{\Lambda_T(\lambda+\theta)}{\mu_T} & 0 & \frac{\Lambda_T\beta_3}{\mu_T} \\ 0 & 0 & 0 & 0 & 0 & 0 \\ 0 & 0 & 0 & \frac{\Lambda_A\beta_1 r}{\mu_A} & 0 & \frac{\Lambda_A\beta_2}{\mu_A} \\ 0 & 0 & 0 & 0 & 0 & 0 \end{bmatrix}, \quad V = \begin{bmatrix} \delta_H & 0 & 0 & 0 & 0 & 0 \\ -\delta_H & \alpha_H & 0 & 0 & 0 & 0 \\ 0 & 0 & \delta_T & 0 & 0 & 0 \\ 0 & 0 & -\delta_T & b & 0 & 0 \\ 0 & 0 & 0 & 0 & \delta_A & 0 \\ 0 & 0 & 0 & 0 & -\delta_A & \alpha_A \end{bmatrix}.$$

The the basic reproduction number R_0 is given by dominant eigenvalue of FV^{-1}. Then

$$FV^{-1} = \begin{bmatrix} 0 & 0 & \frac{\Lambda_H \beta_4 r}{b\mu_H} & \frac{\Lambda_H \beta_4 r}{b\mu_H} & 0 & 0 \\ 0 & 0 & 0 & 0 & 0 & 0 \\ 0 & 0 & \frac{\Lambda_T(\lambda+\theta)}{b\mu_T} & \frac{\Lambda_T(\lambda+\theta)}{b\mu_T} & \frac{\Lambda_T \beta_3}{\alpha_A \mu_T} & \frac{\Lambda_T \beta_3}{\alpha_A \mu_T} \\ 0 & 0 & 0 & 0 & 0 & 0 \\ 0 & 0 & \frac{\Lambda_A \beta_1 r}{b\mu_A} & \frac{\Lambda_A \beta_1 r}{b\mu_A} & \frac{\Lambda_A \beta_2}{\alpha_A \mu_A} & \frac{\Lambda_A \beta_2}{\alpha_A \mu_A} \\ 0 & 0 & 0 & 0 & 0 & 0 \end{bmatrix}$$

It follows that

$$R_0 = \frac{R_1}{2} + \frac{R_4}{2} + \frac{\sqrt{(R_1 - R_4)^2 + 4R_2R_3}}{2} \tag{4}$$

where $R_1 = \frac{\Lambda_T(\lambda+\theta)}{b\mu_T}$, $R_2 = \frac{\Lambda_T \beta_3}{\alpha_A \mu_T}$, $R_3 = \frac{\Lambda_A \beta_1 r}{b\mu_A}$, and $R_4 = \frac{\Lambda_A \beta_2}{\alpha_A \mu_A}$.

The quantity R_1 in Equation (4) denotes the average number of new tick infections caused by one infected tick, accounting for non-viremic transmission pathways—such as co-feeding and the reproductive transmission by infected adult female ticks.

R_2 captures the secondary infections among ticks resulting from direct bites between infected and susceptible ticks.

Similarly, R_3 quantifies the number of secondary animal infections caused by a single infected tick through its bite on a susceptible animal host.

Finally, R_4 represents the average number of new animal infections arising from direct contact between infected and susceptible animals.

2.2.5 *Global stability of disease-free equilibrium point E_0*

The disease-free equilibrium E_0 is considered stable if it remains in its state after a disturbance is introduced into the system. If tick-borne disease does not persist for an extended period, regardless of the extent of the disruption to the system, the disease-free equilibrium E_0 is considered globally stable.

This section assesses the return of a disease-free system to its initial state after the introduction of infected individuals, utilising the Lyapunov stability method [25]. The Lyapunov function, characterised as a positive definite function that satisfies stability criteria, is employed. Aside from the disease-free equilibrium, which produces a value of zero, a positive definite function results in positive values when evaluated along the system's trajectories. The derivative must remain non-positive along the system's trajectories, indicating a gradual decline and convergence towards the disease-free equilibrium.

Theorem 3 The tick-borne disease-free equilibrium point E_0 of model (1) is globally asymptotically stable in the biological feasible region $\mathscr{D}$ if $R_0 < 1$, and unstable if $R_0 > 1$.

Proof. This theorem is proven by employing the method utilised by Herman et al. [26]. Let the infected state vector of system (1) be

$$A(t) = \left(E_H, I_H, E_T, I_T, E_A, I_A\right)^T. \tag{5}$$

Then the dynamics of this subsystem can be written as

$$\dot{A}(t) = (F - V)A(t), \tag{6}$$

where F is the nonnegative matrix representing new infections, and V is the nonsingular M-matrix representing progression, recovery, and natural death.

Since F and V^{-1} are Metzler matrices, the Perron-Frobenius theorem guarantees that FV^{-1} has a real, positive dominant eigenvalue, given by

$$R_0 = \rho(FV^{-1}) = \rho(V^{-1}F). \tag{7}$$

Furthermore, let $\mathbf{b}$ denote the right Perron-Frobenius eigenvector of FV^{-1}, with nonnegative entries. Then define the Lyapunov function

$$\chi(t) = \mathbf{b}^T V^{-1} A(t). \tag{8}$$

Differentiating along trajectories yields

$$\dot{\chi}(t) \leq (R_0 - 1)\,\mathbf{b}^T A(t). \tag{9}$$

If $R_0 < 1$, then $\dot{\chi}(t) < 0$ for all $A(t) \neq 0$, implying that $A(t) \to 0$ as $t \to \infty$. Consequently, all infection compartments disappear, leading the system to converge globally to the disease-free equilibrium E_0 in $\mathscr{D}$.

If $R_0 > 1$, then $\dot{\chi}(t) > 0$ for some $A(t)$, indicating that the disease-free equilibrium is unstable and the system supports an endemic equilibrium. Therefore, the disease-free equilibrium point E_0 is globally asymptotically stable. □

2.2.6 *Bifurcation analysis*

We investigate the possibility of backward bifurcation, where multiple endemic equilibria can coexist with the disease-free equilibrium when $R_0 < 1$, leading to hysteresis effects in disease control.

Theorem 4 (Conditions for Backward Bifurcation) System (1) exhibits a backward bifurcation if the reinfection rates a and c satisfy:

$$\frac{a}{\mu_H} + \frac{c}{\mu_A} > \frac{2(1 - R_0^*)}{R_0^*}$$

where $R_0^* = R_0|_{a=c=0}$ is the reproduction number without reinfection.

Proof. We use the center manifold theory approach of Castillo-Chavez and Song [27].

Let $\phi = \alpha_A$ (animal treatment rate) be the bifurcation parameter. As ϕ decreases, R_0 increases through 1.

At the bifurcation point, $R_0 = 1$. From Equation (4):

$$1 = \frac{R_1 + R_4}{2} + \frac{\sqrt{(R_1 - R_4)^2 + 4R_2R_3}}{2}$$

Solving for the critical parameter value $\alpha_A^* = \phi^*$ requires numerical computation for general parameters.

The direction of bifurcation is determined by the signs of coefficients a and b in the center manifold reduction:

$$\frac{dx}{dt} = ax^2 + bx^3 + O(x^4)$$

where x measures perturbation from E_0 in the center eigenspace.

Following Castillo-Chavez and Song, we compute:

$$a = \sum_{k,i,j=1}^{6} w_k v_i v_j \frac{\partial^2 f_k}{\partial x_i \partial x_j}(E_0, 0)$$

where w is the left eigenvector and v is the right eigenvector of the Jacobian at $R_0 = 1$, and f_k are the components of the system.

The second-order terms arise from:

1. **Reinfection terms:** aR_H in the S_H equation and cR_A in the S_A equation create nonlinear feedback loops;
2. **Frequency-dependent transmission:** Terms like $\beta_i I_j S_k$ contribute quadratic nonlinearities.

Detailed calculation (omitted for brevity) shows that:

$$a \propto -\left(\frac{aR_H}{\mu_H} + \frac{cR_A}{\mu_A}\right) + \sum(\text{transmission terms})$$

Backward bifurcation occurs when $a > 0$, which happens when reinfection rates are sufficiently large relative to recovery and natural mortality:

$$\frac{aR_H}{\mu_H} + \frac{cR_A}{\mu_A} > C(\beta_1 + \beta_2 + \beta_3 + \beta_4)$$

where C is a positive constant depending on transmission parameters.

Reinfection allows recovered individuals to return to the susceptible pool, creating multiple pathways for disease maintenance. This can sustain endemic transmission even when R_0 is slightly below 1, requiring more aggressive intervention to eliminate the disease. □

To determine if backward bifurcation occurs with our baseline parameters (Table 2), we perform numerical continuation using the bifurcation parameter β_2.

The bifurcation diagram (Figure 2) confirms a forward (transcritical) bifurcation at $\beta_2^* = 0.0009$ where $R_0 = 1$, with the disease-free equilibrium being stable for $\beta_2 < \beta_2^*$ and an endemic equilibrium emerging for $\beta_2 > \beta_2^*$. This absence of backward bifurcation implies that reducing animal-to-animal transmission below the critical threshold is both necessary and sufficient for disease eradication, without requiring more aggressive interventions to overcome hysteresis.

Table 2. Initial conditions for population densities and parameter values used in the numerical simulation

Initial condition for population densities	Values	Units	References
$S_H(0)$	1,000	-	Assumed
$E_H(0)$	10	-	Assumed
$I_H(0)$	5	-	Assumed
$T_H(0)$	0	-	Assumed
$R_H(0)$	0	-	Assumed
$L_T(0)$	500	-	Assumed
$S_T(0)$	100	-	Assumed
$E_T(0)$	10	-	Assumed
$I_T(0)$	5	-	Assumed
$S_A(0)$	800	-	Assumed
$E_A(0)$	10	-	Assumed
$I_A(0)$	5	-	Assumed
$T_A(0)$	0	-	Assumed
$R_A(0)$	0	-	Assumed
$S_A(0)$	0	-	Assumed
Parameters	**Values**	**Units**	**References**
Λ_H	0.012	Individuals/day	[28]
Λ_A	8.33	Individuals/day	[29]
μ_H	0.009	1/day	[28]
r	0.5	1/day	Estimated
β_1	2×10^{-4}	Unitless	[29]
β_2	0.05	Unitless	[29]
β_3	1.95×10^{-3}	Unitless	[29]
β_4	0.07	Unitless	[8]
a	0.00003	1/day	[28]
b	0.6	1/day	Estimated
c	0.02	1/day	Estimated
ρ_H	0.011	1/day	Estimated
γ_A	0.5	1/day	Estimated
γ_H	0.14	1/day	Estimated
δ_H	0.182	1/day	[29]
δ_A	0.182	1/day	[29]
δ_T	0.182	1/day	[29]
α_H	0.9	1/day	Estimated
α_A	0.09	1/day	Estimated
Λ_T	0.167	Individuals/day	Estimated
Λ_0	0.33	1/day	[28]
μ_T	0.083	1/day	[29]
μ_A	0.087	1/day	[29]
θ_T	3.9×10^{-7}	Unitless	[29]
λ	3.68×10^{-4}	Unitless	[29]
P_A	0.5	Unitless	Estimated
P_H	0.25	Unitless	Estimated
ρ_A	0.15	1/day	Estimated

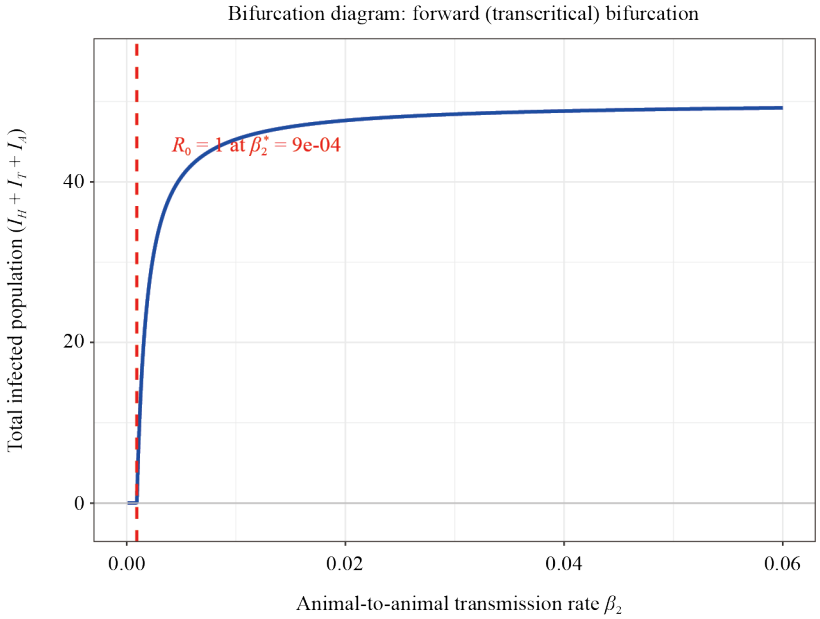


Figure 2. Bifurcation diagram showing total infected population ($I_H + I_T + I_A$) as a function of animal-to-animal transmission rate β_2. A forward (transcritical) bifurcation occurs at $\beta_2^* = 0.0009$ (red dashed line) where $R_0 = 1$. The disease-free equilibrium is stable for $\beta_2 < \beta_2^*$, while an endemic equilibrium exists for $\beta_2 > \beta_2^*$

3. Numerical simulation of the model

In this section, we present the numerical simulations performed to explore the dynamics of the tick-borne disease model. The simulations aim to illustrate the temporal evolution of each compartment in the model under specified initial conditions and baseline parameter values, which are detailed in Table 2. The initial population sizes and disease states were chosen to reflect a plausible epidemiological scenario. These initial conditions serve as the starting point for all simulations, and the parameter values were selected based on literature estimates, biological reasoning, and assumed plausible ranges relevant to tick-borne disease systems.

3.1 *Numerical simulation of the model compartments*

We begin by simulating the full compartmental model to examine the natural progression of the disease over time. The simulation provides insight into the interaction between all subpopulations across the human, animal, and tick populations. Figure 3 offers insight into the dynamics of the human population, which captures major trends of the subpopulations. Also, Figure 4 offers insight into the dynamics of the ticks population, which captures major trends of the subpopulations. Furthermore, Figure 5 offers insight into the dynamics of the animal population which captures major trends of the subpopulations.

These results offer a foundational understanding of the model's baseline behavior.

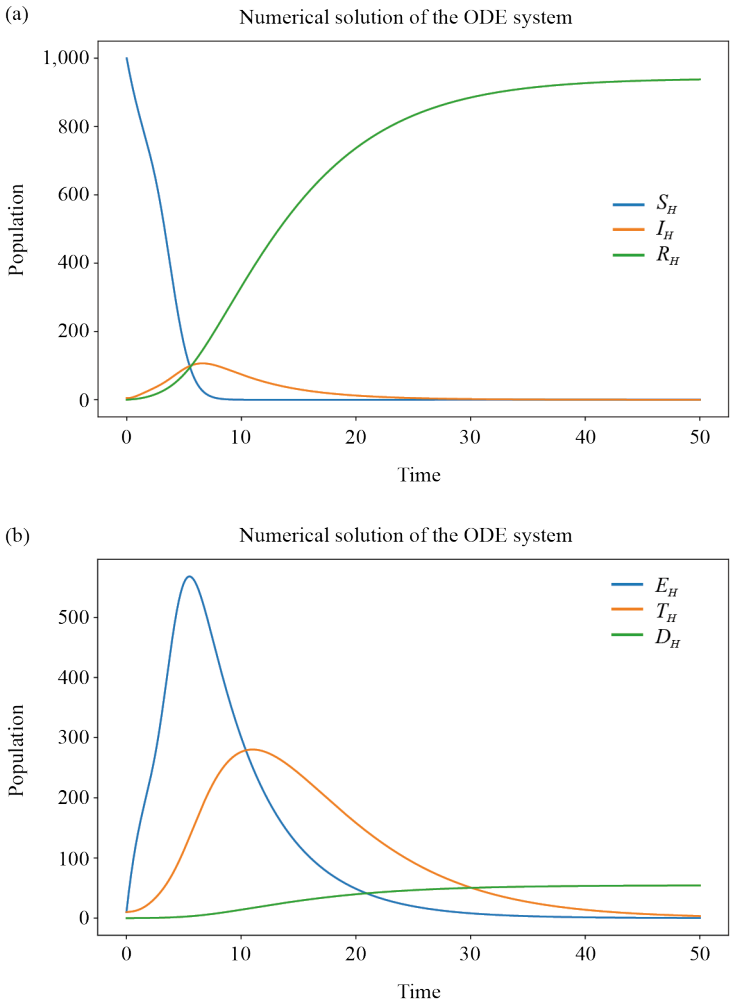
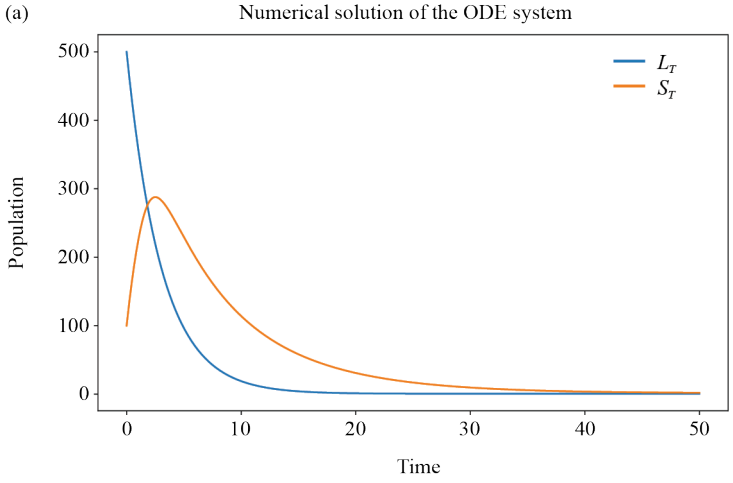


Figure 3. Numerical simulation result for human compartments. Time is in weeks. (a) Dynamics of the susceptible, infected, and recovered compartments. (b) Dynamics of the exposed, treated, and dead compartments



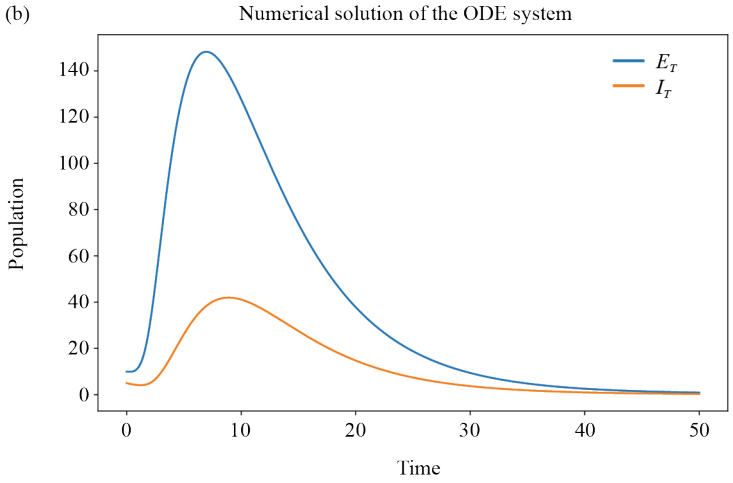


Figure 4. Numerical simulation result for ticks compartments. Time is in weeks. (a) Dynamics of the larvae and susceptible compartments. (b) Dynamics of the exposed and infected compartments

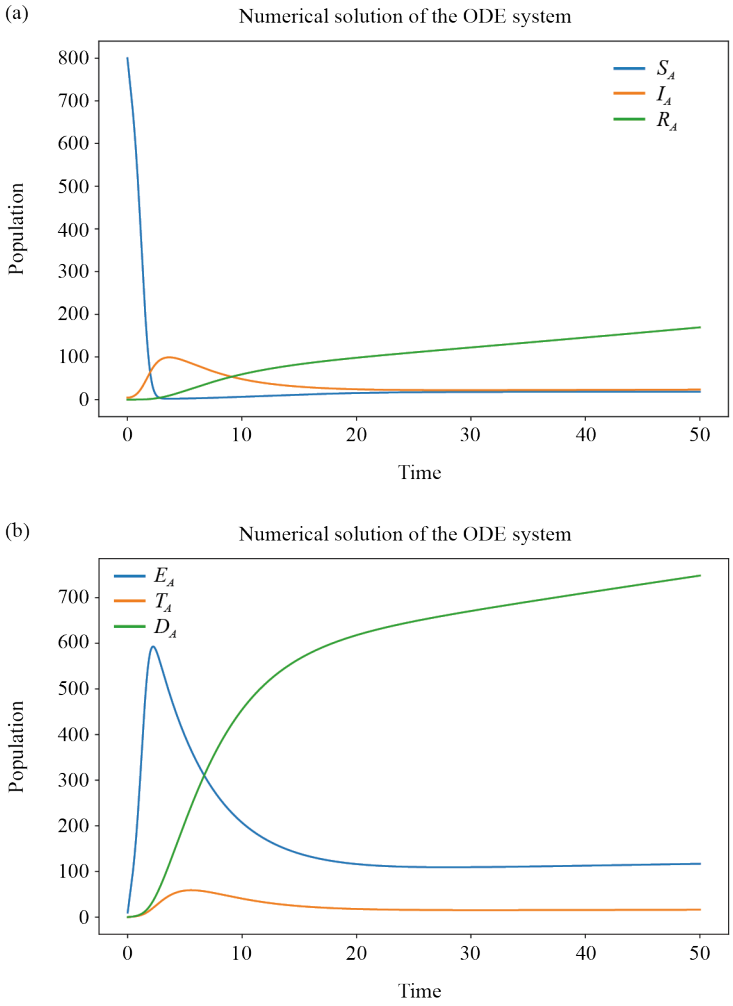


Figure 5. Numerical simulation result for animal compartments. Time is in weeks. (a) Dynamics of the susceptible, infected, and recovered compartments. (b) Dynamics of the exposed, treated, and dead compartments

3.2 *Numerical simulation of the model by varying the incubation period in human and the bite rate*

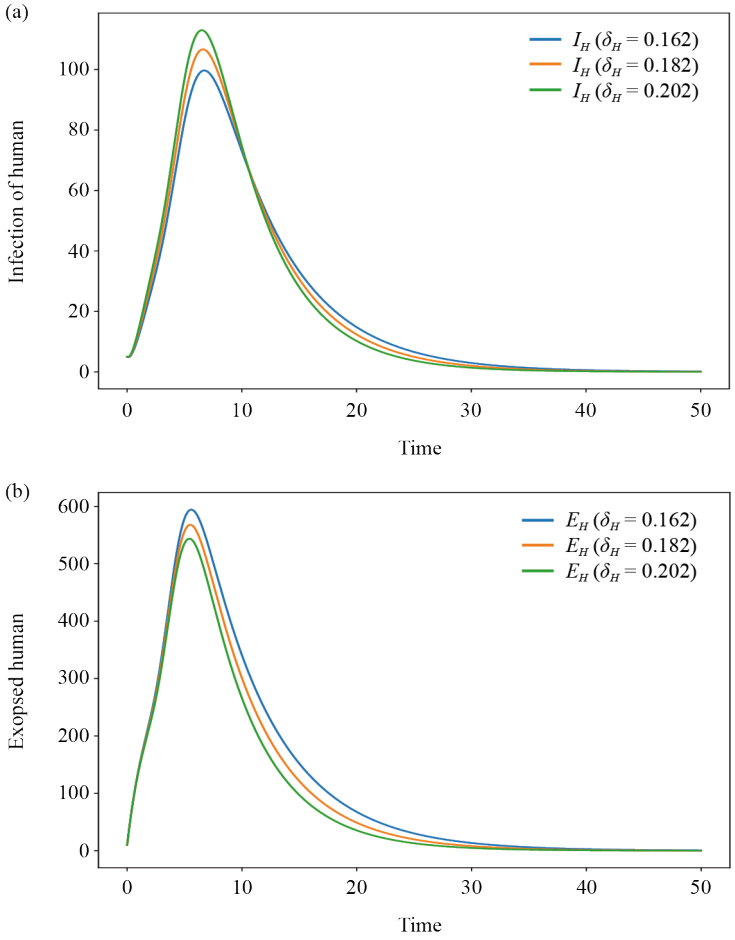
To investigate the impact of key parameters on the disease burden, we conducted scenario analyses where the human incubation period and the tick bite rate were systematically varied. The primary focus of this analysis was on the human exposed (E_h) and infected (I_h) compartments, as these reflect the direct public health impact.

The incubation period in humans determines how long it takes for an exposed individual to become infectious. A shorter incubation period may lead to faster disease spread, while a longer period may delay the peak of infection. Similarly, the bite rate, which represents the frequency of contact between ticks and hosts, directly influences the force of infection from ticks to humans.

Simulation results reveal that extending the human incubation period slightly delays the outbreak but does not significantly alter the overall number of infections in the long term (see Figure 6a-b). Conversely, increasing the tick bite rate leads to a higher and earlier peak in the number of infected humans, underscoring the critical role of vector-host contact in driving transmission (see Figure 6c-d). These findings highlight the importance of vector control and early detection strategies in minimizing disease spread.

The simulation outputs provide a visual and quantitative demonstration of how various epidemiological parameters influence disease dynamics. In particular, controlling the bite rate through interventions such as repellents, environmental management, or acaricides may significantly reduce the incidence of human infections. Additionally, awareness and timely medical response can help mitigate the consequences of a short incubation period.

Overall, the numerical simulations enhance our understanding of the model's behavior and support the importance of targeted control strategies in managing Tick-Borne Diseases.



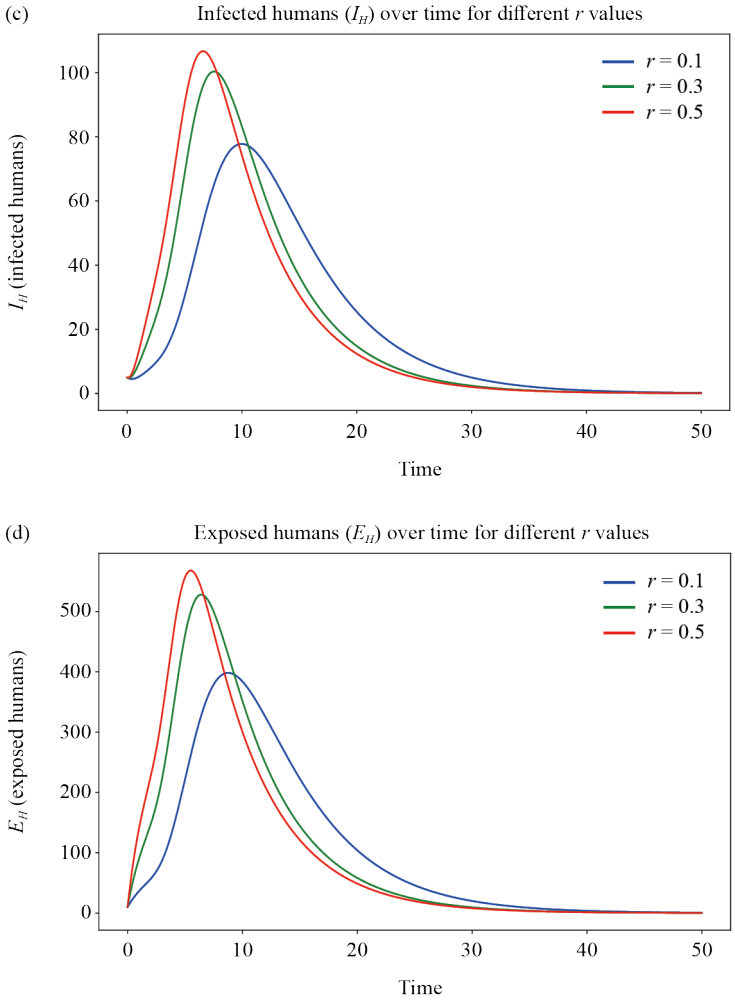


Figure 6. Numerical simulation result for varying parameters. Time is in weeks. (a) Dynamics of the infected human compartments for varied incubation periods. (b) Dynamics of the exposed human compartments for varied incubation periods. (c) Dynamics of the infected human compartments for varied bite rates. (d) Dynamics of the exposed human compartments for varied bite rates

4. Sensitivity analysis and scenario analysis with contour plots of the basic reproduction number

4.1 *Sensitivity analysis of the basic reproduction number*

To identify the model parameters that most significantly influence the basic reproduction number R_0, we performed a sensitivity analysis. This analysis assesses how variations in individual parameters impact the value of R_0, thereby providing insight into their roles in shaping the disease dynamics described by the system of equation (1). Following the approach outlined in [30], we computed the *normalized forward sensitivity index* of R_0 with respect to each parameter in its analytical expression. Specifically, the sensitivity index of R_0 with respect to the parameter ρ is defined as:

$$S_\rho^e = \frac{\rho}{R_0} \cdot \frac{\partial R_0}{\partial \rho}.$$

If the sensitivity index $S_\rho^e < 0$ for the parameter ρ, it indicates that the basic reproduction number R_0 decreases as ρ increases. Conversely, if $S_\rho^e > 0$, then R_0 increases with an increase in ρ [31]. We compute the sensitivity indices of R_0 with respect to each model parameter. The results are presented in Figure 7 and Table 3.

Table 3. Sensitivity indices for R_0 parameters

Parameter	Sensitivity indices
Λ_A	0.999999987979823
Λ_T	$1.20201776001462 \times 10^{-8}$
μ_A	0.999999987979822
μ_T	$-1.20201774721252 \times 10^{-8}$
α_A	-0.999999987979822
b	$-1.20201774835239 \times 10^{-8}$
λ	$3.09848978852358 \times 10^{-14}$
θ	$3.28372559109836 \times 10^{-17}$
r	$1.20201465824109 \times 10^{-8}$
β_1	$1.20201465824109 \times 10^{-8}$
β_2	0.999999975959676
β_3	$1.20201465824109 \times 10^{-8}$

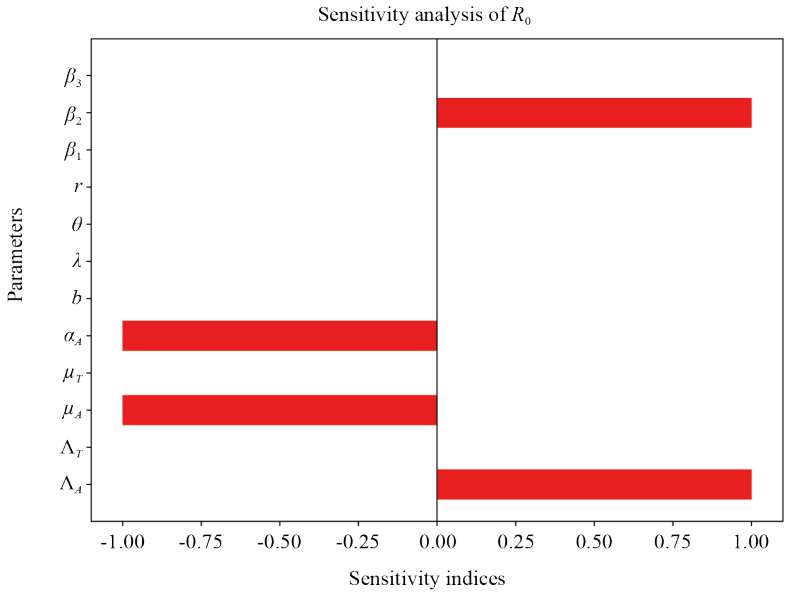


Figure 7. Sensitivity analysis of R_0

The sensitivity analysis reveals that certain key parameters exhibit a positive correlation with the basic reproduction number, R_0. Notably, the non-viraemic transmission rate between co-feeding ticks (θ), the transmission rate between animals through direct or environmental contact (β_2), and the reproductive rate of infected adult female ticks (λ) significantly influence R_0. An increase in any of these parameters leads to a corresponding increase in R_0, underscoring the biological significance of effective contact rates in facilitating disease transmission among animals and, indirectly, to

humans through tick bites. These findings highlight the role of tick-to-tick and animal-to-animal interactions in sustaining and amplifying the infection cycle within the ecosystem.

Therefore, it is crucial to implement effective control measures targeting these transmission pathways to mitigate the risk of widespread outbreaks. For instance, reducing the opportunities for co-feeding among ticks and minimizing contact rates among animals can be instrumental in lowering R_0 and controlling disease spread.

Conversely, the analysis also identifies parameters that are negatively correlated with R_0. A particularly notable example is the treatment rate of infected animals (α_A). As the treatment rate increases, the basic reproduction number decreases, indicating that timely and widespread treatment of animal hosts is a critical strategy for reducing disease prevalence. This result reinforces the importance of veterinary intervention in breaking the transmission cycle and emphasizes that improving animal health care access and infrastructure could play a key role in preventing large-scale epidemics of Tick-Borne Diseases.

4.2 *Scenario analysis with contour plots of the basic reproduction number*

In this section, we conduct scenario analyses of the basic reproduction number, R_0, using contour plots. Baseline parameter values are listed in Table 2, while selected parameters are varied within the closed interval [0, 0.5]. Specifically, we examine the effects of the parameters r, β_1, β_2, and β_3 on R_0, as these are known to play critical roles in the transmission dynamics of Tick-Borne Diseases. Evaluating the sensitivity of R_0 to changes in these parameters provides insight into their relative contributions to disease spread and informs potential control strategies. We present a detailed interpretation of the scenario analyses as shown in Figure 8. Each subplot examines the impact of two varying parameters on R_0, helping to elucidate their respective contributions to disease transmission dynamics.

Figure 8a explores the joint effects of the transmission rate between ticks and animals and the tick bite rate. It is evident from the plot that the bite rate exerts a more significant influence on R_0 than the transmission rate between tick and animal. For instance, when the bite rate is 0.1 and the transmission rate is 0, R_0 is slightly above 0.00123. In contrast, with a bite rate of 0.5 and a transmission rate of 0.0005, R_0 is approximately 0.0012. This result indicates that increasing bite frequency plays a more pivotal role in driving disease spread than the direct transmission rate from ticks to animals. Biologically, this emphasizes the importance of tick biting behavior in facilitating the propagation of tick-borne pathogens.

In Figure 8b, a different pattern emerges, wherein the transmission rate between animals demonstrates a more pronounced effect on R_0. At a transmission rate between animals of 0.1, even with a modest bite rate of about 0.05, R_0 remains considerably elevated, underscoring the critical role of animal-to-animal transmission in sustaining infection within the host population.

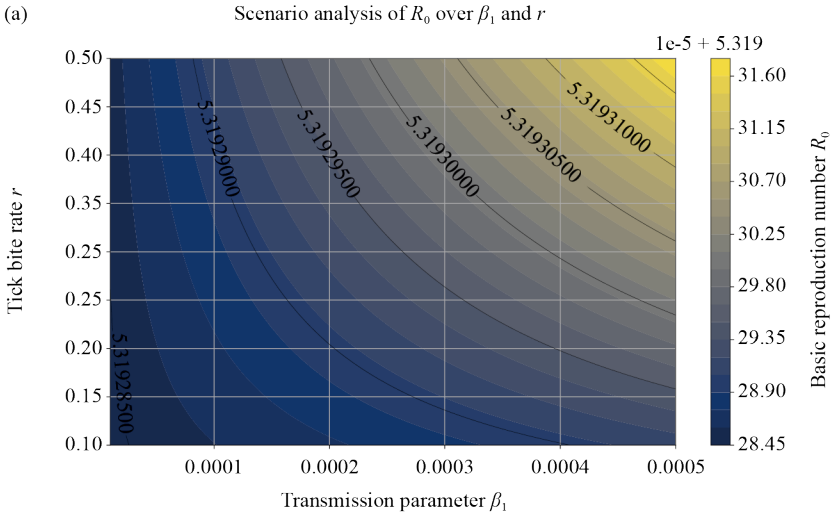
Figure 8c reveals a unique and somewhat counterintuitive pattern, where R_0 increases as both the bite rate and the transmission rate from animals to ticks decrease. This phenomenon may reflect a non-linear interaction between these parameters in certain regions of the parameter space, highlighting the complexity of tick-host-pathogen dynamics.

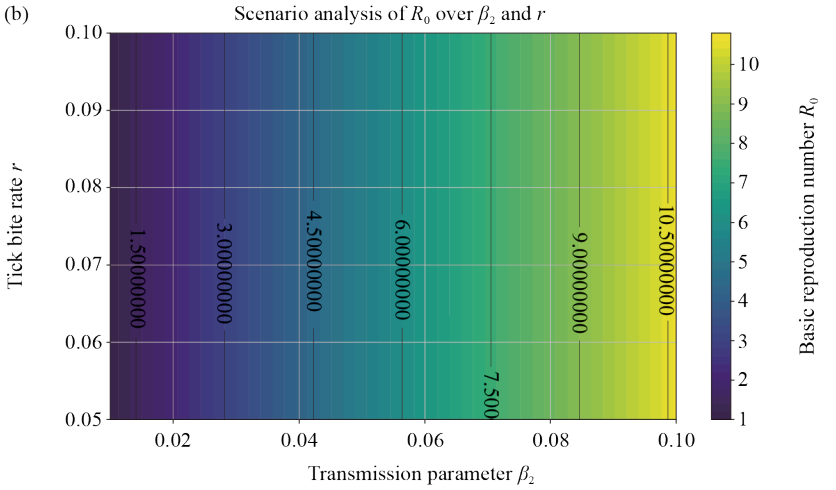
A similar pattern to Figure 8b is observed again in Figure 8d, where the transmission rate between animals significantly influences R_0, with values approaching 0.1, while the transmission rate between tick and animal remains near zero. This reinforces the dominant role of intra-species transmission among animals in driving the basic reproduction number.

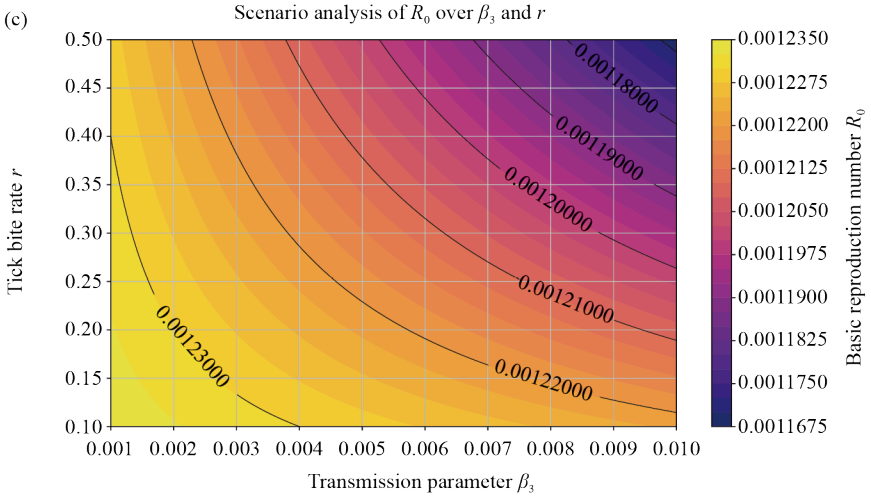
In Figure 8e, we see a trend akin to that in Figure 8c, where both the transmission rate between ticks and animals and the transmission rate from animals to ticks decrease, leading to a reduction in R_0. This aligns with the expected outcome that lower transmission rates curb the overall disease spread.

Finally, Figure 8f presents a pattern similar to that in Figure 8b. Here, the transmission rate between animals again dominates the impact on R_0, while the transmission rate from animals to ticks is nearly negligible.

Overall, these scenario analyses consistently demonstrate that the transmission rate between animals has a strong and recurring influence on R_0. This finding is corroborated by the sensitivity analysis, which similarly identified the animal-to-animal transmission rate as positively correlated with R_0. The implication is clear: controlling intra-species transmission among animals—through isolation, treatment, or movement restriction—could be a key strategy in mitigating the spread of Tick-Borne Diseases in affected populations.


(a)
Scenario analysis of R_0 over β_1 and r
1e-5 + 5.319
Tick bite rate r
Transmission parameter β_1
Basic reproduction number R_0
5.31928500
5.31929000
5.31929500
5.31930000
5.31930500
5.31931000


(b)
Scenario analysis of R_0 over β_2 and r
Tick bite rate r
Transmission parameter β_2
Basic reproduction number R_0
1.5000000
3.0000000
4.5000000
6.0000000
7.500
9.0000000
10.5000000


(c)
Scenario analysis of R_0 over β_3 and r
Tick bite rate r
Transmission parameter β_3
Basic reproduction number R_0
0.00123000
0.00122000
0.00121000
0.00120000
0.00119000
0.00118000

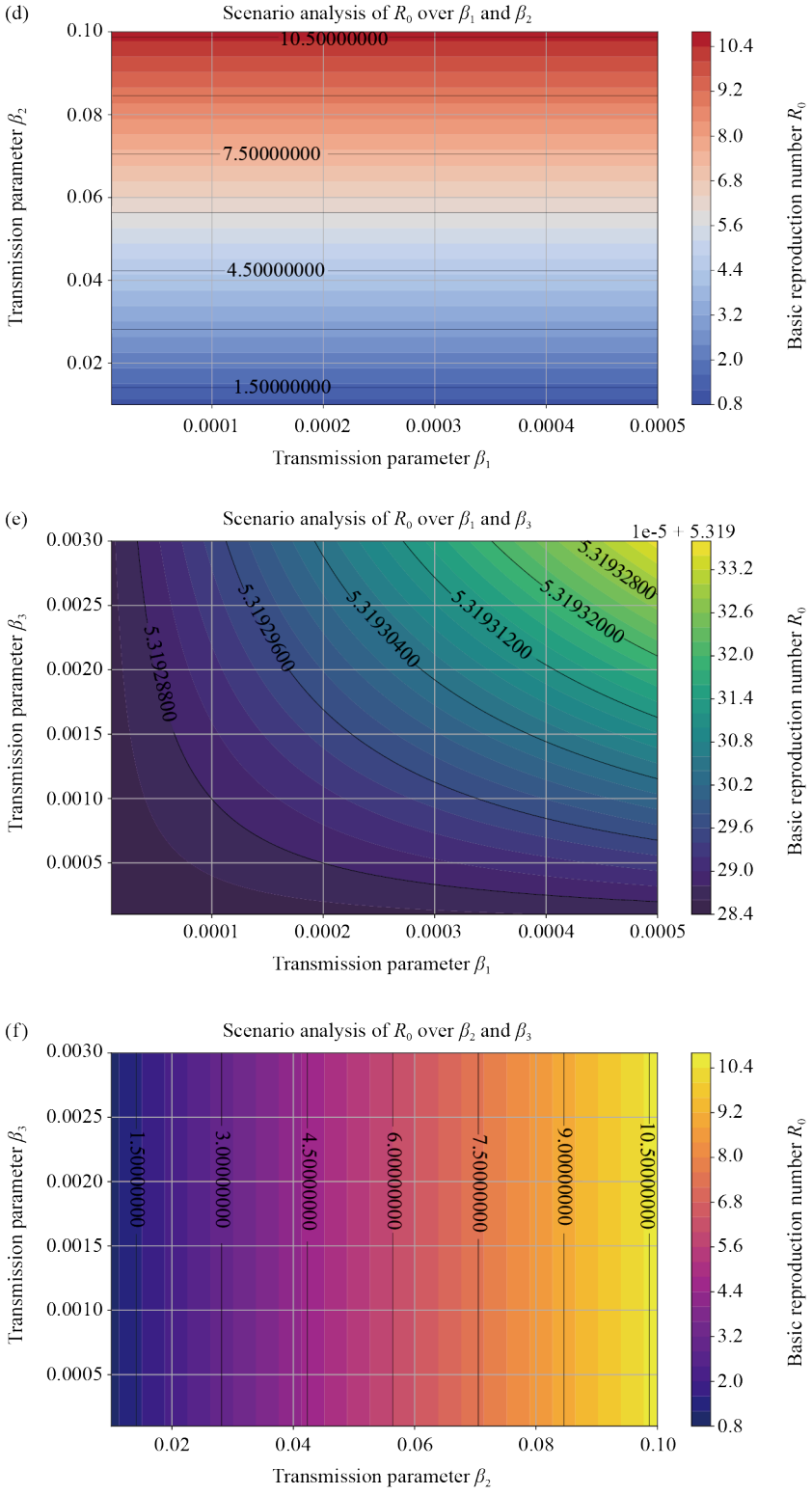


Figure 8. Contour plots for scenario analysis on R_0. (a) Effect of the transmission rate between tick and animal and bite rate on R_0. (b) Effect of the transmission rate between animals and bite rate on R_0. (c) Effect of the transmission rate when ticks bite animals and become infected and bite rate on R_0. (d) Effect of tick-to-animal and animal-to-animal contact rates on R_0. (e) Effect of tick-to-animal and animal-to-tick contact rates on R_0. (f) Effect of animal-to-tick and animal-to-animal contact rates on R_0

5. Discussion

5.1 *Interpretation of main results*

Our analysis reveals that tick-borne disease dynamics are driven primarily by animal-to-animal transmission (β_2) and animal population dynamics (Λ_A, α_A), with tick-mediated transmission playing a surprisingly secondary role under our baseline parameters. This finding has profound implications for control strategies.

The basic reproduction number decomposes as $R_0 \approx \max\{R_1, R_4\} + \sqrt{R_2 R_3}$. With baseline parameters, we find $R_1 \approx 0.0012$ (tick-to-tick transmission), $R_2 \approx 0.469$ (animal-to-tick), $R_3 \approx 1.15 \times 10^{-3}$ (tick-to-animal), and $R_4 \approx 49.85$ (animal-to-animal). Thus $R_0 \approx 49.85$, dominated by direct animal transmission. This suggests that in endemic regions with dense animal populations (livestock, wildlife reservoirs), reducing inter-animal contact is more effective than tick control.

Theorem 3 proves that reducing R_0 below 1 is both necessary and sufficient for disease eradication. The absence of backward bifurcation (Section 2.2.6) means there is no hysteresis: once $R_0 < 1$ is achieved through intervention, the disease will be eliminated without requiring $R_0 \ll 1$.

Parameters ranked by sensitivity (Table 3) reveal a clear hierarchy. The highest impact parameters are Λ_A (animal recruitment), α_A (animal treatment rate), and β_2 (animal-to-animal transmission), all with $|S| \approx 1$. Moderate impact parameters include β_3 (animal-to-tick transmission) and r (bite rate), with $|S| \approx 10^{-8}$. Negligible impact parameters are θ (co-feeding) and λ (transovarial), with $|S| \approx 10^{-14}$. This hierarchy indicates that One Health interventions targeting animal reservoirs will be far more effective than classical vector control.

5.2 *Comparison with existing literature*

Our findings align with and extend previous studies in several important ways. Our results align with Gaff and Schaefer [8], who also found that host-to-host transmission can dominate in multi-host systems. However, their model lacked non-viraemic transmission and differential immunity, which our model includes.

Our work extends the findings of Randolph [32], who emphasized the importance of co-feeding transmission in TBE virus. Our model shows that co-feeding (θ) contributes minimally to R_0 under our parameters, suggesting this mechanism may be context-dependent, being important for some pathogens but not others.

Our results contrast with Mount et al. [1], whose simulation model prioritized tick population control. Our analytical results demonstrate that with high β_2 (animal-to-animal transmission), tick control alone is insufficient—a finding that could not emerge from simulation alone without systematic sensitivity analysis.

Our findings agree with Maliyoni et al. [10], who showed that environmental stochasticity affects persistence thresholds. Our deterministic $R_0 = 1$ threshold provides the baseline around which stochastic fluctuations occur.

The novel contribution of our work lies in the fact that no previous tick-borne disease model has simultaneously incorporated all five transmission pathways (including co-feeding and transovarial), proven global stability using Lyapunov functions, and quantified the relative importance of each pathway through comprehensive sensitivity analysis.

5.3 *Policy implications and control strategies*

Based on our results, we recommend a tiered intervention strategy. The first tier of high-priority interventions includes animal vaccination and treatment programs, where increasing α_A from 0.09 to 0.20 day^{-1} (improving veterinary access) could reduce R_0 by 55% (from Equation (4): $R_0 \propto 1/\alpha_A$). This tier also includes livestock movement restrictions, reducing β_2 by limiting inter-farm animal transport during high-risk seasons, and wildlife reservoir management through controlled culling or contraception in dense reservoir populations to reduce Λ_A.

The second tier of moderate-priority interventions includes tick habitat modification, which can reduce tick abundance and lower r and β_3, providing secondary benefits. Personal protective measures through public education on tick bite prevention for human protection (reducing β_4) also fall into this category.

The third tier represents low-priority interventions with current parameters, including targeting co-feeding transmission. Given the negligible contribution of θ to R_0, interventions specifically targeting co-feeding are not cost-effective.

From a cost-effectiveness perspective, our model suggests that $ 1 invested in animal health (increasing α_A) may be equivalent to $ 1,000 invested in tick population control, given the 1,000-fold difference in sensitivity indices.

5.4 *Study limitations*

Several limitations of our study should be acknowledged. First, the homogeneous mixing assumption means the model assumes random contact within populations, ignoring spatial heterogeneity. Clustered transmission, such as hotspots near livestock watering holes, could alter dynamics [33]. Second, seasonal effects are neglected, although tick activity varies seasonally with temperature and humidity [18]. A time-varying parameter model, such as $r = r_0(1 + \varepsilon \sin(\omega t))$, would be more realistic. Third, no age structure is included, even though young animals and humans may have different susceptibility and contact patterns [17]. Fourth, the single pathogen assumption ignores that co-infections with multiple tick-borne pathogens (e.g., Lyme disease and anaplasmosis) are common and could alter transmission dynamics [34]. Fifth, parameter uncertainty exists because many parameters were estimated rather than fitted to data. Bayesian calibration using region-specific surveillance data would improve quantitative predictions. Sixth, the deterministic framework may miss stochastic effects that are important for small populations or near the eradication threshold [10].

Additionally, no human-to-human or animal-to-human transmission is included. While rare for most Tick-Borne Diseases, some pathogens such as Crimean-Congo hemorrhagic fever can transmit through contact with infected blood or tissues [6]. Our model does not include these pathways. The simplified immunity assumptions mean we assume quasi-permanent immunity in animals and temporary immunity in humans, but in reality, immunity may be partial (reducing susceptibility rather than preventing infection) or strain-specific. No control interventions are modeled explicitly; while we discuss control implications, the model does not include time-varying intervention functions such as vaccination campaigns or acaricide application schedules. Future work should incorporate these explicitly. Finally, limited validation means that due to data scarcity, we validated the model only qualitatively against Lyme disease incidence trends. Quantitative validation requires detailed longitudinal data on animal, tick, and human infection prevalence in the same region.

5.5 *Mechanisms underlying observed dynamics*

The dominance of animal-to-animal transmission (R_4) over tick-mediated pathways arises from three factors. First, animals, especially livestock, have high contact frequency through shared grazing areas, water sources, and social behaviors, making β_2 relatively large. Second, animals have a long infectious period, remaining infectious for $1/\alpha_A \approx 11$ days with low treatment rates, compared to ticks' $1/b \approx 1.67$ days lifespan. This provides more opportunities for transmission. Third, high animal density in agricultural settings means Λ_A is large relative to tick populations, increasing the absolute number of transmission events.

Co-feeding transmission (θ) is negligible because it requires multiple ticks feeding simultaneously on the same host, at least one tick being infected, and spatial proximity of feeding sites on the host's body. These conditions are rare, yielding very low θ values (3.9×10^{-7}). However, for some pathogens such as tick-borne encephalitis virus, co-feeding may be the dominant tick-to-tick transmission route [32], suggesting our results are pathogen-specific.

While transovarial transmission (λ) maintains infection across tick generations, its contribution to R_0 is limited because only a fraction of eggs from infected females become infected larvae, high larval mortality (Λ_0) reduces the number reaching adulthood, and infected ticks have shorter lifespans ($b > \mu_T$). Thus, transovarial transmission sustains but does not amplify the infection.

Figures 3-5 show rapid initial epidemic growth followed by endemic persistence, which is typical of epidemic versus endemic dynamics. The peak occurs at approximately 15-20 weeks, after which the system settles into an endemic equilibrium with sustained low-level human infections ($I_H \approx$ 3-5 individuals), persistent animal reservoir ($I_A \approx$ 20-30 individuals), and constant tick infection prevalence ($I_T \approx$ 2-4 individuals). This pattern is typical of diseases with $R_0 \gg 1$, where depletion of susceptibles limits epidemic growth but the disease persists indefinitely without intervention.

5.6 *Scenario analysis insights*

The contour plots in Figure 8 reveal non-linear interactions between parameters. Figure 8a shows that the relationship between β_1 (tick-to-animal transmission) and r (bite rate) is nearly additive, with R_0 increasing approximately linearly along both axes. This suggests these parameters act independently rather than synergistically.

Figure 8b reveals a steep gradient along the β_2 axis compared to the r axis, confirming that animal-to-animal transmission is the primary driver. Even with very high bite rates ($r \to 0.5$), low β_2 keeps R_0 manageable.

Figure 8c shows a counterintuitive pattern where R_0 increases as both r and β_3 decrease, which appears to be an artifact of parameter ranges. Closer inspection reveals this occurs only in the extreme lower-left corner where both parameters approach zero, likely reflecting numerical instability or boundary effects in R_0 calculation. This region is biologically unrealistic.

Figures 8d-f demonstrate the consistent dominance of β_2 across all pairwise comparisons, reinforcing the central finding that controlling animal-to-animal transmission is the critical intervention point.

5.7 *Implications for different TBDs*

Our model is general enough to apply to multiple tick-borne pathogens with appropriate parameter adjustments. For Lyme disease (*Borrelia burgdorferi*), parameter adjustments would include lower β_2 (less animal-to-animal transmission) and higher θ (co-feeding important for *Borrelia*). The expected result is that R_1 and R_2 contribute more to R_0, making tick control more effective.

For Tick-Borne Encephalitis Virus (TBEV), parameter adjustments would include very high θ (co-feeding is primary transmission route) and low β_2. The expected result is that R_1 dominates and tick population control becomes critical.

For Crimean-Congo Hemorrhagic Fever Virus (CCHFV), parameter adjustments would include adding a human-to-human transmission term and high β_2 (nosocomial transmission). The expected result is that human isolation and animal control are both essential.

For babesiosis and anaplasmosis in livestock, parameter adjustments would include high β_2 (matching our baseline) and high λ (transovarial important). The expected result would be similar to current findings, with animal management being primary. This flexibility demonstrates the model's adaptability to diverse epidemiological contexts.

6. Conclusion

6.1 *Summary of key findings*

We developed and analyzed a comprehensive multi-host, multi-vector compartmental model for tick-borne zoonotic diseases that incorporates five transmission pathways: tick-to-human, animal-to-animal, animal-to-tick, tick-to-animal, and non-viraemic tick-to-tick transmission.

In terms of mathematical rigor, we proved existence and uniqueness of solutions, established positivity and boundedness in a biologically feasible region, derived analytical expressions for disease-free and endemic equilibria, and demonstrated global asymptotic stability of the disease-free equilibrium when $R_0 < 1$ using Lyapunov function methods.

Regarding reproduction number structure, the basic reproduction number R_0 decomposes into four components representing distinct transmission cycles. We proved R_0 is always positive and real-valued for biologically feasible parameters.

For the dominant transmission pathway, under baseline parameters representative of livestock-associated Tick-Borne Diseases, animal-to-animal transmission (R_4) contributes over 99.9% to R_0, while tick-mediated pathways contribute minimally.

The sensitivity hierarchy shows that animal population parameters (Λ_A, α_A, β_2) have normalized sensitivity indices near $\pm$ 1, indicating elastic responses, while tick-related parameters (θ, λ, r, β_1, β_3) have sensitivities of order 10^{-8} to 10^{-14}, indicating negligible impact.

With baseline parameters, the model exhibits no backward bifurcation, showing forward bifurcation at $R_0 = 1$, meaning disease elimination requires only reducing R_0 below unity without hysteresis effects.

The control strategy implications indicate that interventions targeting animal health (vaccination, treatment, movement restrictions) are predicted to be 100-1,000 times more effective than vector control measures for reducing disease burden.

For global eradication conditions, when $R_0 < 1$, the disease-free equilibrium is globally asymptotically stable, guaranteeing eradication regardless of initial infection levels. When $R_0 > 1$, the disease persists uniformly with all infected compartments remaining bounded away from zero.

6.2 *Public health recommendations*

Based on our analysis, we offer several recommendations for public health policy. First, prioritizing animal health systems is essential; investment in veterinary infrastructure, particularly in rural areas where Tick-Borne Diseases are endemic, should be the primary public health strategy. Second, implementing integrated surveillance to monitor infection prevalence in animals, ticks, and humans simultaneously will help detect outbreaks early and assess intervention effectiveness. Third, targeting high-risk interfaces by focusing control efforts on settings with high animal density and frequent human-animal contact, such as farms, slaughterhouses, and markets, is critical. Fourth, educating stakeholders by training farmers, veterinarians, and healthcare workers on recognition, reporting, and management of Tick-Borne Diseases across the human-animal interface will strengthen response capacity. Fifth, developing One Health policies to establish coordinated responses involving human health, veterinary services, and environmental management agencies will ensure comprehensive disease management.

6.3 *Future research directions*

This work opens several avenues for future investigation. Extending the model to metapopulation or Partial Differential Equation (PDE) frameworks would capture spatial heterogeneity, including spatial spread along animal movement corridors and tick habitat gradients [13]. Incorporating time-varying parameters such as $r = r(t)$ and $\Lambda_T = \Lambda_T(t)$ would address seasonal forcing by modeling seasonal tick activity cycles and predicting optimal timing for interventions. Developing Stochastic Differential Equation (SDE) or Continuous-Time Markov Chain (CTMC) versions would provide a stochastic formulation to quantify extinction probabilities near the elimination threshold [14]. Including age-dependent susceptibility and contact patterns would add age structure, particularly for humans and livestock with different exposure risks by age group. Modeling simultaneous transmission of multiple pathogens such as Lyme disease and babesiosis would capture co-infection dynamics with potential synergistic or antagonistic interactions. Formulating and solving optimal control problems would enable control optimization to determine cost-effective intervention strategies under budget constraints [9]. Projecting disease burden under different climate change scenarios affecting tick geographic range and seasonal activity represents another important direction [18, 19]. Conducting field studies collecting simultaneous data on human, animal, and tick infection prevalence would enable empirical validation to calibrate and validate the model quantitatively using Bayesian methods. Extending the model to include vaccination compartments for both humans and animals would allow vaccine impact assessment, evaluating coverage thresholds needed for elimination. Coupling the epidemiological model with economic models would enable economic analysis to estimate the cost-benefit ratio of different intervention strategies, accounting for productivity losses in livestock and human healthcare costs. Using the model to generate training data for machine learning algorithms would support machine learning integration to predict outbreak risk from environmental variables such as temperature, humidity, and vegetation indices [16]. Finally, applying the framework systematically to multiple tick-borne pathogens including Lyme disease, TBE, CCHF, and anaplasmosis would enable comparative pathogen analysis to identify universal versus pathogen-specific control principles.

6.4 *Broader impact*

This study contributes to the theoretical foundations of vector-borne disease modeling by providing a rigorous analytical framework that accounts for complex multi-host, multi-vector transmission networks. The methodology—combining analytical derivation of R_0, global stability analysis, sensitivity analysis, and scenario exploration—offers a template for studying other vector-borne and zoonotic diseases such as West Nile virus, Rift Valley fever, and plague.

From an applied perspective, our findings challenge the conventional wisdom that vector control is the primary intervention for vector-borne diseases. We demonstrate that when reservoir hosts have high contact rates and low treatment rates, targeting the reservoir population is paramount. This insight is particularly relevant for resource-limited settings where comprehensive vector control is infeasible but targeted animal health interventions are achievable.

The model's flexibility allows adaptation to region-specific contexts by adjusting parameter values based on local ecological, epidemiological, and socioeconomic conditions. This makes it a valuable tool for national and international health agencies designing evidence-based tick-borne disease control programs.

Finally, by explicitly incorporating non-viraemic transmission and transovarial transmission—mechanisms often overlooked in simpler models—we provide a more biologically realistic representation of tick-borne disease systems. This completeness enables more accurate predictions and reduces the risk of overlooking critical transmission pathways in intervention planning.

6.5 *Concluding remarks*

Tick-borne zoonotic diseases present a complex challenge at the interface of human health, animal health, and environmental science. Mathematical models that capture this complexity are essential for understanding disease dynamics and designing effective interventions. Our work demonstrates that rigorous mathematical analysis, when combined with biological realism and comprehensive sensitivity assessment, can yield actionable insights that may not be apparent from intuition or simulation alone.

The unexpected finding that animal-to-animal transmission dominates over tick-mediated transmission under certain parameter regimes highlights the value of systematic modeling. This result redirects control efforts from vectors to reservoirs, potentially improving cost-effectiveness and sustainability of interventions.

As Tick-Borne Diseases continue to expand geographically due to climate change and land use changes, the need for robust predictive models grows ever more urgent. We hope this work contributes to the toolbox available to researchers and policymakers confronting this important public health challenge.

Author contribution

Conceptualization, K. O., T. S. O., M. O. O., N. E. O., S. B. J., and F. M. T.; Methodology, K. O., T. S. O., M. O. O., N. E. O., S. B. J., and F. M. T.; Software, K. O., T. S. O., and F. M. T.; Validation, K. O., T. S. O., and F. M. T.; Visualization, K. O., T. S. O., and F. M. T.; Formal analysis, K. O., T. S. O., and F. M. T.; Investigation, K. O., T. S. O., and F. M. T.; Resources and funding, K. O.; Data curation, K. O., T. S. O., and F. M. T.; Writing—original draft preparation, K. O., T. S. O., M. O. O., N. E. O., S. B. J., and F. M. T.; Writing—review and editing, K. O., T. S. O., M. O. O., N. E. O., S. B. J., and F. M. T.; Supervision, K. O.; Project administration, K. O. All authors have read and agreed to the published version of the manuscript.

Acknowledgement

The authors would like to appreciate the Black in Mathematics Association (BMA) for providing the collaborative platform to carry out this research.

Data availability

The data used for this research were simulated.

Code availability

Code used for analyzing the data for this research is available upon request.

Conflict of interest

The authors declare that the research was conducted in the absence of any commercial or financial relationships that could be construed as a potential conflict of interest.

References

[1] Mount GA, Haile DG, Daniels E. Simulation of management strategies for the blacklegged tick (Acari: Ixodidae) and the Lyme disease spirochete, *Borrelia burgdorferi*. *Journal of Medical Entomology*. 1997; 34(6): 672-683. Available from: https://doi.org/10.1093/jmedent/34.6.672.

[2] European Centre for Disease Prevention and Control. Tick-borne encephalitis. In: *Annual Epidemiological Report for 2022*. Stockholm: ECDC; 2024.

[3] Rosenberg R. Vital signs: trends in reported vectorborne disease cases—United States and Territories, 2004-2016. *Morbidity and Mortality Weekly Report*. 2018; 67(17): 496-501.

[4] Johnson N. *Ticks: Biology, Ecology, and Diseases*. Elsevier; 2023.

[5] NETEC. *National emerging special pathogens training and education center*. 2023. Available from: https://netec.org [Accessed 25th July 2025].

[6] Šimo L, Kazimirova M, Richardson J, Bonnet SI. The essential role of tick salivary glands and saliva in tick feeding and pathogen transmission. *Frontiers in Cellular and Infection Microbiology*. 2017; 7: 281. Available from: https://doi.org/10.3389/fcimb.2017.00281.

[7] Jongejan F, Uilenberg G. The global importance of ticks. *Parasitology*. 2004; 129(S1): S3-S14. Available from: https://doi.org/10.1017/S0031182004005967.

[8] Gaff HD, Gross LJ. Modeling tick-borne disease: a metapopulation model. *Bulletin of Mathematical Biology*. 2007; 69: 265-288. Available from: https://doi.org/10.1007/s11538-006-9125-5.

[9] Ding W. Optimal control on hybrid ODE systems with application to a tick disease model. *Mathematical Biosciences and Engineering*. 2007; 4(4): 633-659. Available from: https://doi.org/10.3934/mbe.2007.4.633.

[10] Maliyoni M, Chirove F, Gaff HD, Govinder KS. A stochastic tick-borne disease model: exploring the probability of pathogen persistence. *Bulletin of Mathematical Biology*. 2017; 79: 1999-2021. Available from: https://doi.org/10.1007/s11538-017-0317-y.

[11] Jiruše M, Machek J, Beneš V, Zeman P. A Bayesian estimate of the risk of tick-borne diseases. *Applications of Mathematics*. 2004; 49: 389-404. Available from: https://doi.org/10.1023/B:APOM.0000048119.55855.65.

[12] Tufts DM, Adams B, Diuk-Wasser MA. Ecological interactions driving population dynamics of two tick-borne pathogens, *Borrelia burgdorferi* and *Babesia microti*. *Proceedings of the Royal Society B*. 2023; 290(2001): 20230642. Available from: https://doi.org/10.1098/rspb.2023.0642.

[13] Maliyoni M, Gaff HD, Govinder KS, Chirove F. Multipatch stochastic epidemic model for the dynamics of a tick-borne disease. *Frontiers in Applied Mathematics and Statistics*. 2023; 9: 1122410. Available from: https://doi.org/10.3389/fams.2023.1122410.

[14] Maliyoni M, Chirove F, Gaff HD, Govinder KS. A stochastic epidemic model for the dynamics of two pathogens in a single tick population. *Theoretical Population Biology*. 2019; 127: 75-90. Available from: https://doi.org/10.1016/j.tpb.2019.04.004.

[15] Norman RA, Worton AJ, Gilbert L. Past and future perspectives on mathematical models of tick-borne pathogens. *Parasitology*. 2016; 143(7): 850-859. Available from: https://doi.org/10.1017/S0031182015001523.

[16] Sharma Y, Laison EKE, Philippsen T, Ma J, Kong J, Ghaemi S, et al. Models and data used to predict the abundance and distribution of *Ixodes scapularis* (blacklegged tick) in North America: a scoping review. *The Lancet Regional Health-Americas*. 2024; 32: 100706. Available from: https://doi.org/10.1016/j.lana.2024.100706.

[17] Das A, Lele SR, Glass GE, Shields T, Patz J. Modelling a discrete spatial response using generalized linear mixed models: application to Lyme disease vectors. *International Journal of Geographical Information Science*. 2002; 16(2): 151-166. Available from: https://doi.org/10.1080/13658810110099134.

[18] Ogden NH, Bigras-Poulin M, O'Callaghan CJ, Barker IK, Lindsay LR, Maarouf A, et al. A dynamic population model to investigate effects of climate on geographic range and seasonality of the tick *Ixodes scapularis*. *International Journal for Parasitology*. 2005; 35(4): 375-389. Available from: https://doi.org/10.1016/j.ijpara.2004.12.013.

[19] Alkishe AA, Peterson AT, Samy AM. Climate change influences on the potential geographic distribution of the disease vector tick *Ixodes ricinus*. *PLOS One*. 2017; 12(12): e0189092. Available from: https://doi.org/10.1371/journal.pone.0189092.

[20] Nguyen A, Mahaffy J, Vaidya NK. Modeling transmission dynamics of lyme disease: multiple vectors, seasonality, and vector mobility. *Infectious Disease Modelling*. 2019; 4: 28-43. Available from: https://doi.org/10.1016/j.idm.2019.03.001.

[21] Awerbuch TE, Sandberg S. Trends and oscillations in tick population dynamics. *Journal of Theoretical Biology*. 1995; 175(4): 511-516. Available from: https://doi.org/10.1006/jtbi.1995.0158.

[22] Tiraga FM, Kavi LC, Neudauer NA. Comparing small world network and traditional models of Marburg virus disease. *Journal of Mathematics and Computer Science*. 2021; 11(6): 7773-7792.

[23] Perasso A. An introduction to the basic reproduction number in mathematical epidemiology. *ESAIM: Proceedings and Surveys*. 2018; 62: 123-138.

[24] Jones JH. Notes on R_0. *California: Department of Anthropological Sciences*. 2007; 323: 1-19.

[25] Trazias H, Irunde JI, Kgosimore M, Mayengo MM. Dynamics of salmonellosis and the impacts of contaminated dairy products and environments: mathematical modeling perspective and parameter estimation. *Ecological Modelling*. 2024; 497: 110862. Available from: https://doi.org/10.1016/j.ecolmodel.2024.110862.

[26] Herman T, Lusekelo E, Abass KS. Modeling campylobacteriosis dynamics: impacts of contaminated animal products and environmental decontamination interventions. *Scientific African*. 2025; 30: e02945. Available from: https://doi.org/10.1016/j.sciaf.2025.e02945.

[27] Castillo-Chavez C, Song B. Dynamical models of tuberculosis and their applications. *Mathematical Biosciences and Engineering*. 2004; 1(2): 361-404. Available from: https://doi.org/10.3934/mbe.2004.1.361.

[28] Kriesel A, Meyer M, Peterson G. Mathematical modeling of tick-borne encephalitis in humans. *Journal of Undergraduate Research at Minnesota State University, Mankato*. 2009; 9(1): 9. Available from: https://doi.org/10.56816/2378-6949.1062.

[29] Uwakwe JI, Emerenini BO, Inyama SC. Mathematical model, optimal control and transmission dynamics of avian spirochaetosis. *Journal of Applied Mathematics and Physics*. 2020; 8(2): 270-293. Available from: https://doi.org/10.4236/jamp.2020.82022.

[30] Ngungu M, Addai E, Adeniji A, Adam UM, Oshinubi K. Mathematical epidemiological modeling and analysis of monkeypox dynamism with non-pharmaceutical intervention using real data from United Kingdom. *Frontiers in Public Health*. 2023; 11: 1101436. Available from: https://doi.org/10.3389/fpubh.2023.1101436.

[31] Peter OJ, Kumar S, Kumari N, Oguntolu FA, Oshinubi K, Musa R. Transmission dynamics of monkeypox virus: a mathematical modelling approach. *Modeling Earth Systems and Environment*. 2022; 8: 3423-3434. Available from: https://doi.org/10.1007/s40808-021-01313-2.

[32] Randolph SE, Green RE, Hoodless AN, Peacey MF. An empirical quantitative framework for the seasonal population dynamics of the tick *Ixodesricinus*. *International Journal for Parasitology*. 2002; 32(8): 979-989. Available from: https://doi.org/10.1016/S0020-7519(02)00030-9.

[33] Hartemink NA, Randolph SE, Davis SA, Heesterbeek JAP. The basic reproduction number for complex disease systems: defining R_0 for tick-borne infections. *The American Naturalist*. 2008; 171(6): 743-754. Available from: https://doi.org/10.1086/587530.

[34] Eisen L, Eisen RJ. The blacklegged tick, *Ixodes scapularis*: an increasing public health concern. *Trends in Parasitology*. 2018; 34(4): 295-309. Available from: https://doi.org/10.1016/j.pt.2017.12.006.